PHYSICAL REVIEW D VOLUME 18, NUMBER 3 1 AUGUST 1978

Absorption corrections in the one-particle-inclusive production of vector mesons in the triple-Regge region

K. J. M. Moriarty, J. H. Tabor, and A. Ungkitchanukit
Department of Mathematics, Royal Holloway College, Englefield Green, Surrey, TW20 0EX, United Kingdom
(Received 11 October 1976)

Absorption effects are incorporated in a Mueller-Regge model and inclusive vector-meson production in the triple-Regge region is investigated. The invariant cross section $(s/\pi)d^2\sigma/dt\,dM^2$ and the decay density matrices of the produced resonances are studied and compared with the experimental data.

I. INTRODUCTION

In a previous paper[1] the inclusive production of vector and tensor mesons in the triple-Regge region was investigated in the Mueller-Regge formalism with simple poles. It was found that while the qualitative behavior of the differential cross sections were reasonably well accounted for, the normalization was somewhat overestimated and the polarizations of the produced vector mesons simply could not be explained in terms of poles alone. The theoretical evidence for the need of some type of cut correction in inclusive processes comes from the work of Pumplin,[2] in which an absorption model, similar to our own, is derived using the technique of eikonal field theory. This leads to phenomenological results for the inclusive process $\pi^- + p \to \pi^0 + X$ which can be tested experimentally.[2] Additional theoretical work has been carried out by Paige and Sidhu,[3] who then consider the measurable polarization effects for some inclusive hyperon production processes. The data[4] on target asymmetry for the process $\pi^\pm + p_\uparrow \to \pi^\pm + X$ (the subscript $\uparrow$ indicates that the proton is polarized) provides experimental support for the importance of cuts in inclusive processes. The triple-Regge limit for factorizing poles and Pomeron predicts no target asymmetry to leading order in s in the beam fragmentation region and the main contribution to the target asymmetry is expected to arise from cuts.[5] Soffer and Wray[6] and Craigie *et al.*[7] correctly predicted the target asymmetry in $\pi^\pm + p_\uparrow \to \pi^\pm + X$ and $\gamma + p_\uparrow \to \pi^\pm + X$, respectively, using the Mueller-Regge model with cut corrections.

In the present paper, the inclusive production of vector mesons in the triple-Regge region is considered in a Mueller-Regge model with absorption corrections. As in the previous paper[1] the model does not require any free parameters since all the required parameters are fixed from previous extensive studies of two-body processes. In Sec. II the formalism is set up, and the final form of the Mueller-Regge amplitudes is given in the Appendix. This is followed by Sec. III, which contains the discussion and conclusions resulting from a comparison of the model calculations and the experimental data.

II. FORMALISM

The one-particle inclusive cross section is related through Mueller's generalized optical theorem to the forward discontinuity of the $3 \to 3$ amplitude[8] (see Fig. 1)

$$\sum_X \int \prod_{i=1}^{n} \frac{d^3q_i}{(2\pi)^3 2E_i} (2\pi)^4 \delta^4\left(\sum_{i=1}^{n} q_i + p_c - p_a - p_b\right) \sum_K f_{\lambda_c K,\lambda_a \lambda_b} f^*_{\lambda_c' K,\lambda_a' \lambda_b'} = \frac{1}{2i} \mathrm{disc}_{M^2} f_{\lambda_c' \lambda_b' \lambda_a';\lambda_c \lambda_b \lambda_a} .$$

For the inclusive production of vector mesons in the triple-Regge region, with the assumption of M^2 duality, we have the Mueller-Regge diagram of Fig. 2. To evaluate the Mueller-Regge diagram, the currents at the pseudoscalar-meson–vector-meson–Reggeon $(0^-, 1^-, R)$ vertices are taken to be[9]

$$J_5 = -3h\, Q_\lambda (\bar{\phi}_\lambda \phi_5) F ,$$

and

$$J_\mu = \frac{3h}{m} \epsilon_{\mu\nu\kappa\lambda} P_\nu Q_\kappa (\bar{\phi}_\lambda \phi_5)(D + 2S) ,$$

for pseudoscalar- and vector-meson exchanges, respectively, where ϕ_λ and ϕ_5 are the vector and the pseudoscalar wave functions, respectively, P and Q are the sum and the difference of the incoming and outgoing meson momenta, m is the average mass of the incoming and outgoing mesons at the three-particle vertex, h is the vector-meson–pseudoscalar-meson–pseudoscalar-meson coupling constant which is evaluated from the $\rho \to 2\pi$ decay width, and F and $D + 2S$ are the Clebsch-Gordan coefficients.

FIG. 1. Diagrammatic representation of the Mueller generalized optical theorem.

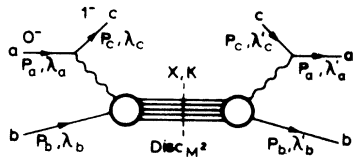

FIG. 2. The Mueller-Regge diagram for the production of vector mesons in the triple-Regge region but with the M^2-large condition relaxed.

The Mueller-Regge diagram (see Fig. 2) gives

$$H^{\lambda_c\lambda_a,\lambda'_c\lambda'_a}_{\lambda_b K,\lambda'_b K}=J^{\lambda_a\lambda_c}_{\mu}\Delta_{\mu\nu}\Gamma^{\lambda_b K}_{\nu}(J^{\lambda'_a\lambda'_c}_{\mu'}\Delta_{\mu'\nu'}\Gamma^{\lambda'_b K}_{\nu'})^{\dagger},$$

for vector exchange and

$$H^{\lambda_c\lambda_a,\lambda'_c\lambda'_a}_{\lambda_b K,\lambda'_b K}=J^{\lambda_a\lambda_c}_{5}\Delta\Gamma^{\lambda_b K}_{5}(J^{\lambda_a\lambda_c}_{5}\Delta\Gamma^{\lambda'_b K}_{5})^{\dagger},$$

for pseudoscalar exchange, where the H's are the Mueller-Regge amplitudes corresponding to Fig. 2 and Δ and Γ are, respectively, the Reggeized propagators and structure functions at the inclusive vertices. Since particle a is a pseudoscalar, the index λ_a is redundant and will be dropped. For the inclusive cross section and polarization calculations for the inclusive vector-meson production we carry out the averaging and the summation, respectively, of λ_b and K, giving

$$\sum_{\lambda_b K}H^{\lambda_c,\lambda'_c}_{\lambda_b K,\lambda_b K}=H^{\lambda_c\lambda'_c}.$$

The structure functions Γ, after averaging and summing over λ_b and K, take the form

$$\sum_{\lambda_b,K}\Gamma^{\lambda_b K}_{5}(\Gamma^{\lambda_b K}_{5})^{*}=2\Delta^{1/2}(M^2,t,m_p{}^2)\sigma_{\text{tot}}(\pi p\to\pi p),$$

for pseudoscalar exchange and for vector exchange we adopt the form [throughout the paper the particle labels (a,b,c) and $(1,2,3)$ are used interchangeably]

$$\sum_{\lambda_b,K}\Gamma^{\lambda_b K}_{\nu}(\Gamma^{\lambda_b K}_{\nu'})^{*}=(p_2)_{\nu}(p_2)_{\nu'}F_V,$$

where

$$F_V=\frac{8m_V{}^2}{M^2}\sigma_{\text{tot}}(Vp\to Vp),$$

with V denoting the exchanged vector meson.

The elastic scattering effect in the initial state shown in Fig. 3(a) is taken into account through absorption in impact-parameter space. In the conventional absorption model with the elastic scattering matrix $S(b)$ we obtain

$$H^{\lambda_c\lambda'_c}_{\text{abs}}(b',b)=S^{*1/2}(b')H^{\lambda_c\lambda'_c}(b',b)S^{1/2}(b).$$

As an *approximation* we take $S^*(b)$ and $S(b)$ to also approximate the rescattering effect in the $\bar{c}b$ channel of Fig. 3(b). Heuristically, it can be seen that in the triple-Regge region $s_{ab}\simeq s_{\bar{c}b}$ and the elastic scattering matrices $S_{ab}(b)$ and $S_{\bar{c}b}(b)$ can be assumed to be roughly equal. Then the absorbed Mueller-Regge amplitudes are approximated by

$$H^{\lambda_c\lambda'_c}_{\text{abs}}(s,\tau,M^2)=\int_0^\infty\tau'd\tau'\int_0^\infty\tau'_1d\tau'_1\int_0^\infty b\,db\,J_\nu(b\tau)J_\nu(b\tau')S(b)$$
$$\times\int_0^\infty b_1db_1J_{\nu'}(b_1\tau)J_{\nu'}(b_1\tau'_1)S^*(b_1)H^{\lambda_c\lambda'_c}(s,\tau',\tau'_1,M^2),$$

where the elastic scattering matrix is given by

$$S=1-Ce^{-\lambda b^2}\simeq\frac{S_{ab}+S_{\bar{c}b}}{2}\simeq S_{ab}{}^{1/2}S_{\bar{c}b}{}^{1/2},$$

with b denoting the impact parameter, C the opacity and $\lambda=R^{-2}$, where R is the interaction radius of the target. In the present study we fix the values of C and λ at 0.7 and 0.068 $(\text{GeV}/c)^2$.

Finally, we obtain

$$H^{\lambda_c\lambda'_c}_{\text{abs}}(s,\tau,M^2)=\int_0^\infty\tau'd\tau'\int_0^\infty\tau'_1d\tau'_1H^{\lambda_c\lambda'_c}(s,\tau',\tau'_1,M^2)$$
$$\times\left[\frac{1}{\tau}\delta(\tau-\tau')-\frac{C}{2\lambda}\exp\left(-\frac{(\tau^2+\tau'^2)}{4\lambda}\right)I_\nu\left(\frac{\tau\tau'}{2\lambda}\right)\right]$$
$$\times\left[\frac{1}{\tau}\delta(\tau-\tau'_1)-\frac{C}{2\lambda}\exp\left(-\frac{(\tau^2+\tau'_1{}^2)}{4\lambda}\right)I_{\nu'}\left(\frac{\tau\tau'_1}{2\lambda}\right)\right].$$

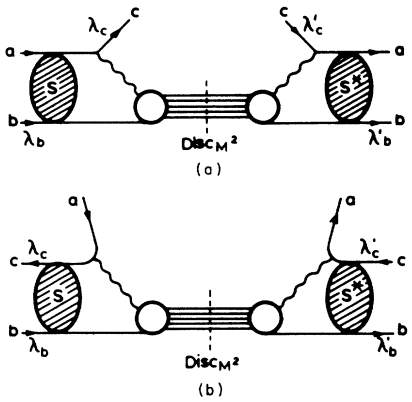

FIG. 3. (a) Rescattering correction to $0^- + p \to 1^- + X$ in the s channel. (b) Rescattering correction to $0^- + p \to 1^- + X$ in the $\bar{c}b$ channel.

The variable τ^2 is defined by $q\tau^2/k = t_{\min} - t$, where k and q are the magnitudes of the c.m. 3-momenta in the initial and final states, respectively, ν and ν' are the total helicity flip on each side of disc_{M^2}. A simplifying assumption that the inclusive vertices are primarily helicity nonflip is made so that ν and ν' are simply λ_c and λ_c'.

In the calculation of $H^{\lambda_c \lambda_c'}$ strong exchange degeneracy is assumed for the particle pairs π-B, ρ-A_2, and ω-f. The trajectory parameters are obtained from the requirement that the trajectories pass through the positions of the particles in the Chew-Frautschi plot and are given in Table I.

The one-particle inclusive cross section is then given by

$$\frac{s}{\pi}\frac{d^2\sigma}{dtdM^2} = \frac{1}{64\pi^2 k^2}\sum_i \sum_{\lambda_c} H_{\text{abs}}^{\lambda_c \lambda_c},$$

where the summation over i indicates the summation over all possible exchanges.

The decay density matrix elements for the vector meson are given by

$$\rho_{\mu'\mu} = \frac{\sum_i H_{\text{abs}}^{\mu'\mu}}{\sum_i \sum_\mu H_{\text{abs}}^{\mu\mu}}.$$

For the decay density matrix elements in the Gottfried-Jackson frame we have

$$\rho_{m'm} = \sum_\mu d^1_{m'\mu'}(\psi_3)\,\rho_{\mu'\mu}\,d^1_{m\mu}(\psi_3),$$

where ψ_3 is the angle between the directions of particles 1 and 4 as seen in the rest frame of particle 3.

III. DISCUSSION AND CONCLUSIONS

The model is applied to the study of the processes $\bar{K}^- + p \to \bar{K}^{*0} + X$ and $\pi^- + p \to \rho^0 + X$ and the results are presented in Figs. 4 to 8. For other $0^- + p \to 1^- + X$ processes the appropriate exchanges and the Clebsch-Gordan coefficients are given in Table II. The exchanges for the process $K^- + p \to \bar{K}^{*0} + X$ are π, B, ρ, and A_2 and for the process $\pi^- + p \to \rho^0 + X$ are π and A_2. Although various experiments for the inclusive production of vector mesons have been reported[10] most of the data is still only qualitative. Detailed data on the inclusive production of vector mesons only exists for the process $K^- + p \to \bar{K}^{*0} + X$ at 14.3 GeV/c.[11] The comparison of the model with the $\bar{K}^{*0}$ production data is presented together with predictions for this process and for ρ^0 production at higher energies.

The inclusive cross sections are given for both fixed M^2 and fixed t while the decay density matrices are given vs t in the Gottfried-Jackson frame. It can be seen in the various diagrams that the inclusive cross sections are well accounted for both in normalization and in structure by the model of the present paper. This is in contrast to the unabsorbed calculation[1] where the normalization was found to be overestimated. For the density matrix elements it can be seen that ρ_{00} and ρ_{1-1} are reasonable, at least in the region of both small $|t|$ and M^2/s. This is the region in which the model is expected to work well. The data for ρ_{00} for $\bar{K}^{*0}$ production seems to agree well with the theoretical prediction for ρ^0 production. Since the ρ^0 production results from the exchange of the π and the A_2 this agreement would indicate that of the expected dominant contributions to ρ_{00} from π and B exchange in $\bar{K}^{*0}$ production, the B exchange term is unimportant.

The fixed t vs M^2/s plots show approximate scaling which is consistent with the experimental results for $\pi^- + p \to \rho^0 + X$ in the P_{lab} range from about 8 GeV/c to 205 GeV/c for the triple-Regge region.[12]

TABLE I. Regge trajectories.

Trajectory	α_0	α' [(GeV/c)$^{-2}$]
π, B	−0.013	0.665
ρ, A_2	0.470	0.905
ω, f	0.386	1.017

TABLE II. Parameters for the Γ-function approximation [obtained by a fit in the range $0 \le |t| \le 2$ (GeV/c)^2].

Exchange	A_1	B_1	A_2	B_2
π, B	−59.891	41.12	−14.143	3.398
ρ, A_2	0.8914	2.96	0.778	−0.072
ω, f	0.8076	2.75	0.645	−0.266

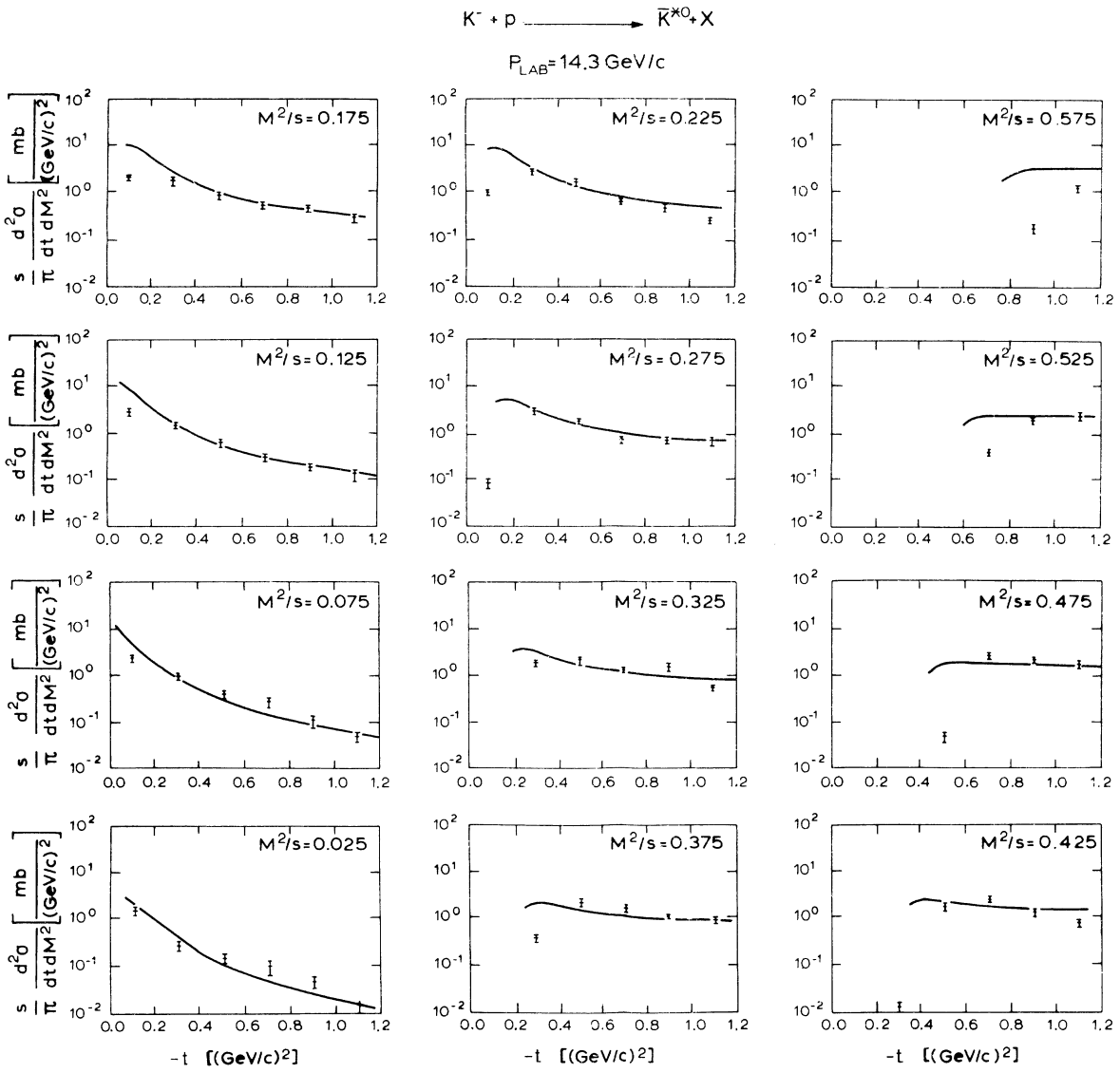

FIG. 4. The inclusive cross section for $K^- + p \to \bar{K}^{*0} + X$ for fixed M^2/s plotted vs t at 14.3 GeV/c. Data are from Ref. 11.

For $K^- + p \to \bar{K}^{*0} + X$ the inclusive total cross section given by

$$\int_{M^2} \int_t \frac{d^2\sigma}{dt dM^2} dt dM^2,$$

for $M^2 = 3.0$ GeV^2 to $M^2 = M_{\max}{}^2$ and $|t| = 0.0005$ to 2.0 (GeV/c)^2 gives the results of 3.02 mb at 14.3 GeV/c and 3.27 mb at 205 GeV/c with most of the increase due to the enlarging of phase space at the higher energy. A similar result is obtained for $\pi^- + p \to \rho^0 + X$; for $M^2 = 5.0$ GeV^2 to $M^2 = M_{\max}{}^2$ and the same limits on $|t|$ we obtain 1.4 mb at 15 GeV/c and 1.5 mb at 205 GeV/c.

The reaction $\pi^\pm + p \to \rho^0 + X$ has been studied using the dual-model B_8 functions. In the dual-model calculation ρ_{00} is found to be important for π exchange[13] but for A_2 exchange[14] ρ_{11} is the dominant decay density matrix element in the present kinematic region. Note that in these dual-model calculations all the possible exchanges are not considered together and no absorption effects are taken into account. For the dual model the inclusive predictions tend to the exclusive predictions as M^2/s decreases. Thus, the dip in ρ_{00} gradually disappears. However, in our model the contrary is predicted, since the absorption effects decrease with M^2 as M^2 increases, the dip in ρ_{00} disappears so ρ_{00} approaches a constant value of 1.

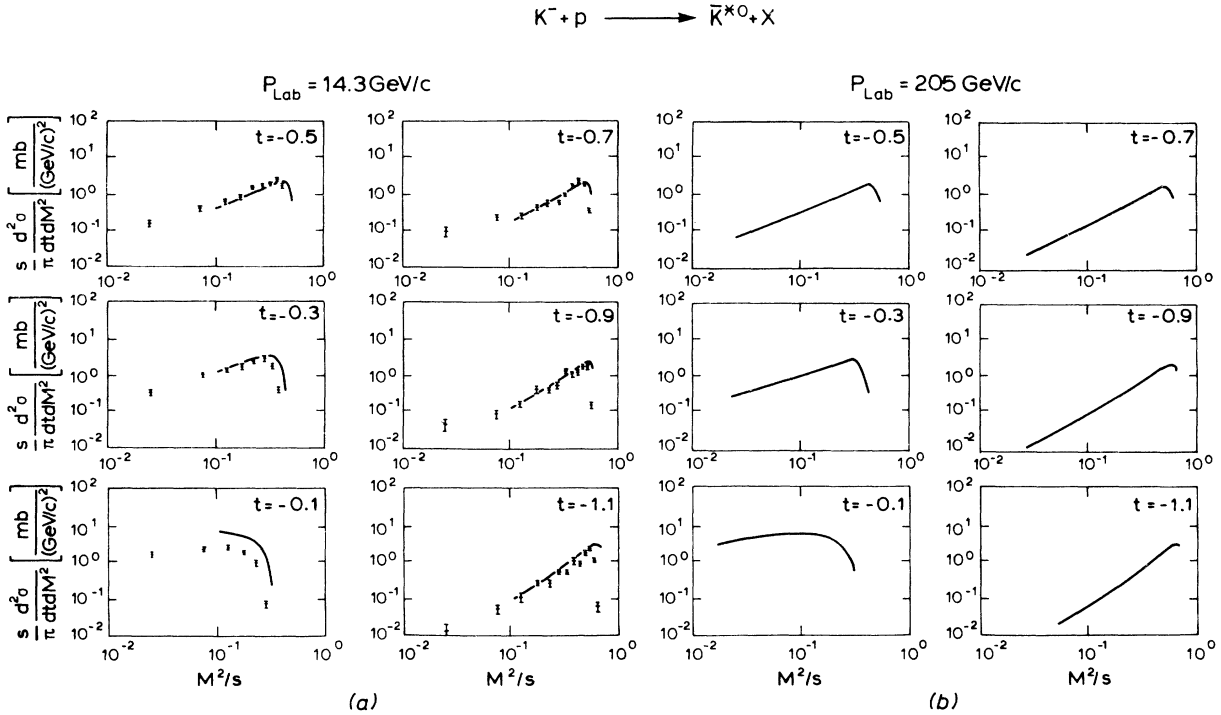

FIG. 5. The inclusive cross section for $K^- + p \to \bar{K}^{*0} + X$ for fixed t plotted vs M^2/s at 14.3 GeV/c and 205 GeV/c. Data at 14.3 GeV/c are from Ref. 11.

To conclude, the present study indicates that Regge-cut corrections are relevant to inclusive production processes. Within the framework of our parameter-free Mueller-Regge model with absorption it is possible to give a reasonable account of the data both qualitatively and quantitatively. However, in a recent paper by Craigie *et al.*[15] it has been indicated that other absorption effects might well be important. Clearly better data are required before stringent tests of the various models become possible.

ACKNOWLEDGMENTS

The support and encouragement of Professor H. G. Eggleston in this work is gratefully acknowledged. We wish to thank J. Randa for helpful comments on the manuscript and R. W. B. Ardill for providing the parameters for the Γ-function fits. One of the authors (A. U.) wishes to thank Royal Holloway College for financial support. Another of the authors (J.H.T.) wishes to thank the Science Research Council for a Research Studentship.

APPENDIX

In this appendix the kinematics and the evaluation of the absorption integrals are presented.

We work in the c.m. frame with the initial- and the final-state 3-momenta given by k and q, respectively. The positive z axis defines the direction of the beam and the reaction plane is taken to be the x-z plane. The direction of the produced particle from the $+z$ axis defines the angle θ, the c.m. scattering angle.

We now consider the evaluation of the absorption integrals. $H^{\lambda_c \lambda_c'}$ can be written in the form

$$H_i^{\lambda_c \lambda_c'} = \Psi_i^{\lambda_c} W_i (\Psi_i^{\lambda_c'})^* ,$$

where i denotes the exchange and

$$\Psi_i^{\lambda_c} = \frac{\alpha_i' \{1 + \xi \exp[-i\pi\alpha_i(t)]\}}{2} \Gamma_i(f(t)) \left(\frac{s}{M^2}\right)^{\alpha_i(t) - J_i} a_i^{\lambda_c} ,$$

where the standard Regge notation is used, $\Gamma_i(f(t))$ are the Euler Γ functions given by

$$\Gamma_i(f(t)) = \begin{cases} -\Gamma(-\alpha_i(t)), & \text{for } i = \text{unnatural parity} \\ \Gamma(1 - \alpha_i(t)), & i = \text{natural parity} , \end{cases}$$

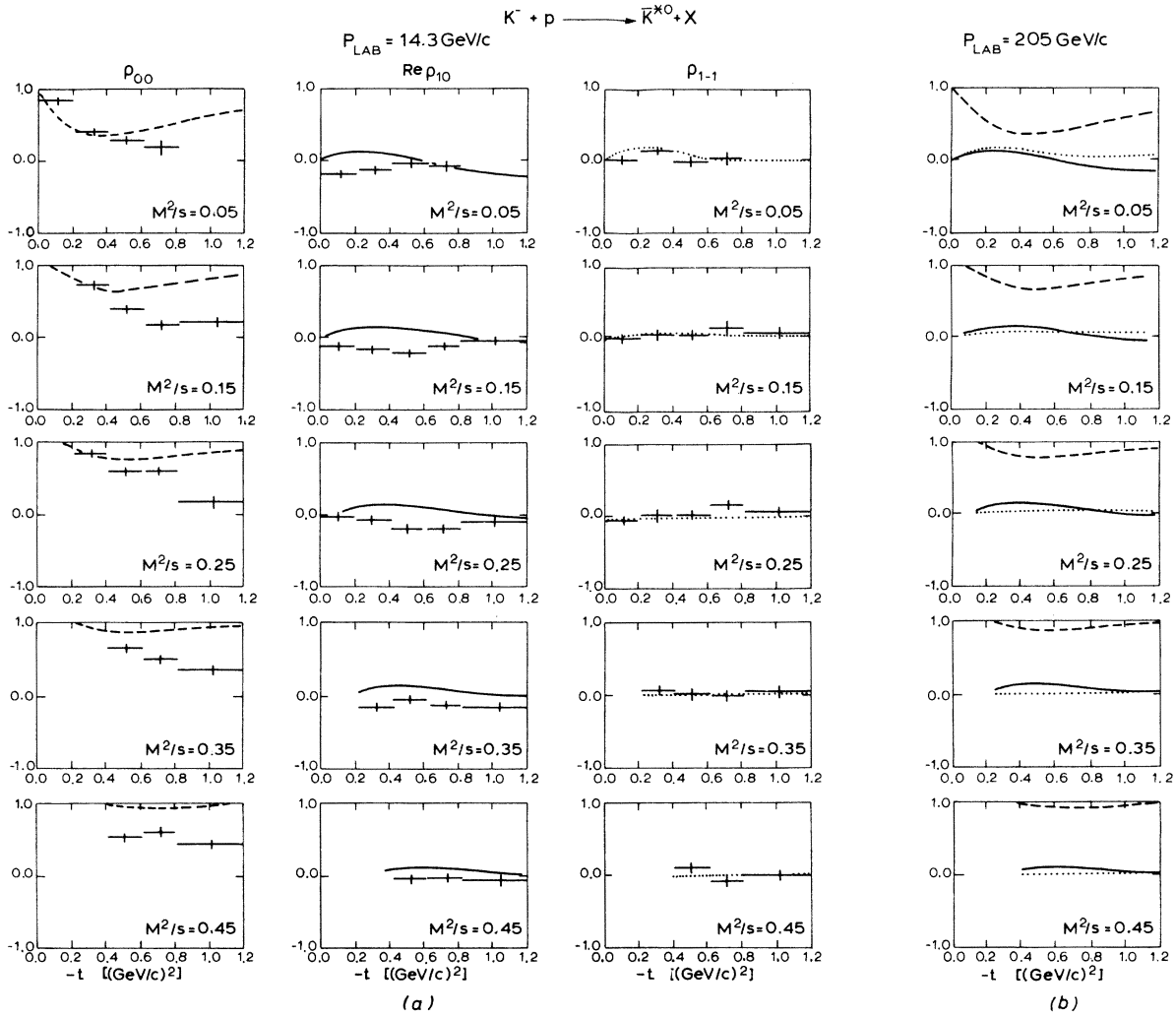

FIG. 6. The density matrix elements for the decay of the $\bar{K}^{*0}$ produced in the reaction $K^- + p \to \bar{K}^{*0} + X$ for fixed M^2/s plotted vs t in the Gottfried-Jackson frame at 14.3 GeV/c and 205 GeV/c. Data at 14.3 GeV/c are from Ref. 11.

where these Γ functions are parameterized in the form

$$\Gamma(f(t)) = A_1 \exp(B_1 t) + A_2 \exp(B_2 t),$$

for analytic solutions of the absorption integrals, with the values of the parameters given in Table III, J_i is the spin of the exchange i and

$$W_i = \begin{cases} (-3hF)^2 2\Delta^{1/2}(M^2, m_2^2, t)\sigma_{\text{tot}}(\pi p), & \text{for } i = \pi \text{ exchange} \\ [3h(D+2S)]^2 \dot{F}_V, & \text{for } i = \text{vector-meson exchange}. \end{cases}$$

The $a_i^{\lambda_c}$ are given by, for pseudoscalar exchange,

$$a_P^0 = \frac{qE_1 - kE_3\cos\theta}{m_3}, \quad a_P^{\pm 1} = \mp \frac{k\sin\theta}{\sqrt{2}},$$

for vector exchange,

$$a_V^0 = 0, \quad a_V^{\pm 1} = \frac{-\sqrt{2}qk(E_1+E_2)\sin\theta}{m_1+m_3}.$$

Using $2k\sin(\theta/2) = \tau$ and writing $H^{\lambda_c \lambda_c'}$, Ψ^{λ_c}, and $(\Psi^{\lambda_c})^*$ in terms of the variable τ (suppressing the variables s and M^2 for the moment) we have

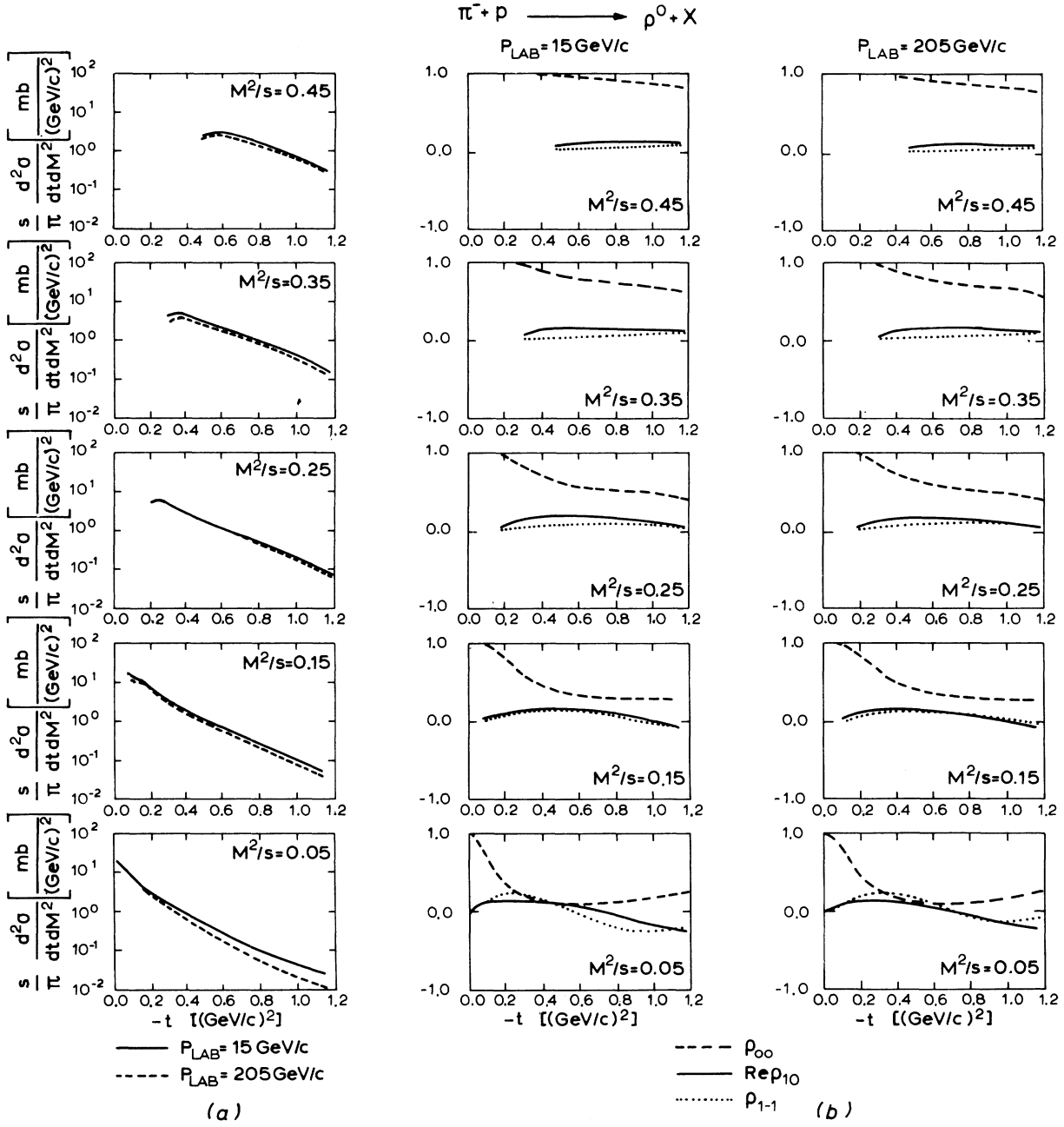

FIG. 7. (a) The inclusive cross section for fixed M^2/s plotted vs t for the reaction $\pi^- + p \to \rho^0 + X$ at 15 GeV/c and 205 GeV/c. (b) The density matrix elements for the decay of the ρ^0 produced in the reaction $\pi^- + p \to \rho^0 + X$ for fixed M^2/s plotted vs t at 15 GeV/c and 205 GeV/c.

$$H^{\lambda_c \lambda_c'}(\tau', \tau_1') = \Psi^{\lambda_c}(\tau')\, W\,[\Psi^{\lambda_c}(\tau_1')]^* .$$

Substituting this in the absorption integral yields

$$H_{\text{abs}}^{\lambda_c \lambda_c'}(\tau) = \left[\Psi^{\lambda_c}(\tau) - \frac{C}{2\lambda}\exp\left(-\frac{\tau^2}{2\lambda}\right)\int_0^\infty \tau' d\tau'\, \Psi^{\lambda_c}(\tau')\exp\left(-\frac{\tau'^2}{4\lambda}\right) I_\nu\left(\frac{\tau\tau'}{2\lambda}\right)\right]$$
$$\times W\left\{[\Psi^{\lambda_c'}(\tau)]^* - \frac{C}{2\lambda}\exp\left(-\frac{\tau^2}{2\lambda}\right)\int_0^\infty \tau_1' d\tau_1' [\Psi^{\lambda_c'}(\tau_1')]^* \exp\left(-\frac{\tau_1'^2}{4\lambda}\right) I_{\nu'}\left(\frac{\tau\tau_1'}{2\lambda}\right)\right\}.$$

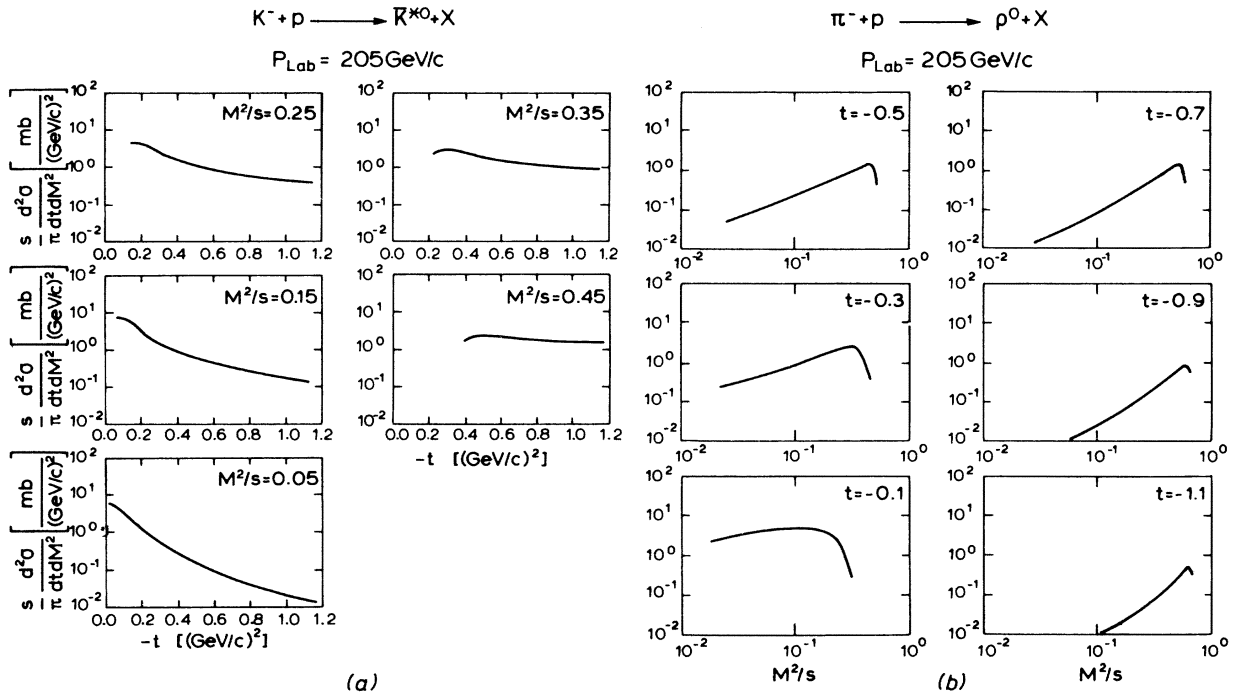

FIG. 8. (a) The inclusive cross section for $K^- + p \to \bar{K}^{*0} + X$ for fixed M^2/s plotted vs t at 205 GeV/c. (b) The inclusive cross section for $\pi^- + p \to \rho^0 + X$ for fixed t plotted vs M^2/s at 205 GeV/c.

This can be put in the form

$$H_{\text{abs}}^{\lambda_c \lambda_c'} = (\Psi^{\lambda_c} - \mathfrak{C}^{\lambda_c}) W [(\Psi^{\lambda_c'})^* - (\mathfrak{C}^{\lambda_c'})^*] .$$

We define the variables

$$\phi_i = \sum_{j=1}^{2} A_i^j \exp(B_i^j t_{\min}) \left(\frac{\alpha_i'}{2}\right) \left(\frac{s}{M^2}\right)^{\alpha_{0_i} + \alpha_i' t_{\min} - J_i} ,$$

$$\zeta_i = \sum_{j=1}^{2} \left\{ \frac{1}{4\lambda} + \left[B_i^j + \alpha_i' \ln\left(\frac{s}{M^2}\right) \right] \frac{q}{k} \right\},$$

$$\zeta_i' = \zeta_i - i\pi\alpha_i'(q/k) ,$$

TABLE III. Clebsch-Gordan coefficients for $0^- + p \to 1^- + X$.

Reaction	Exchange	$D+2S$	F
$\pi^+ + p \to \rho^+ + X$	π, A_2		2
	ω	2	
$\pi^- + p \to \rho^- + X$	π, A_2		−2
	ω	2	
$\pi^- + p \to \rho^0 + X$	π, A_2		2
$\pi^+ + p \to \rho^0 + X$	π, A_2		−2
$\pi^+ + p \to \omega + X$	ρ, B	2	
$K^- + p \to \bar{K}^{*0} + X$	π, A_2		$-\sqrt{2}$
	ρ, B	$\sqrt{2}$	
$K^+ + p \to K^{*0} + X$	π, A_2		$\sqrt{2}$
	ρ, B	$\sqrt{2}$	

$$\chi_i = \frac{\tau^2}{16\lambda^2\zeta_i} ,$$

$$\chi_i' = \frac{\tau^2}{16\lambda^2\zeta_i'} ,$$

$$\eta_i = \xi_i \exp[-i\pi(\alpha_{0_i} + \alpha_i' t_{\min})] ,$$

$$\gamma = \frac{C}{2\lambda} \exp\left(-\frac{\tau^2}{2\lambda}\right).$$

Then the $\mathfrak{C}^{\lambda_c}$ are given by, for pseudoscalar exchange,

$$\mathfrak{C}_P^0 = \frac{\gamma\phi_i}{2m_3} \left\{ \frac{\exp(\chi_i)}{\zeta_i} \left[(qE_1 - kE_3) + \frac{E_3(\chi_i + 1)}{2\zeta_i k} \right] + \eta_i \frac{\exp(\chi_i')}{\zeta_i'} \left[(qE_1 - kE_3) + \frac{E_3(\chi_i' + 1)}{2\zeta_i' k} \right] \right\},$$

$$\mathfrak{C}_P^{\pm 1} = \mp \frac{\gamma\phi_i}{\sqrt{2}} \frac{\tau}{8\lambda} \left[\frac{\exp(\chi_i)}{\zeta_i^2} \left(1 - \frac{\chi_i + 2}{8\zeta_i k^2}\right) + \eta_i \frac{\exp(\chi_i')}{\zeta_i'^2} \left(1 - \frac{\chi_i' + 2}{8\zeta_i' k^2}\right) \right],$$

while for vector exchange,

$$\mathfrak{C}_V^0 = 0 ,$$

$$\mathfrak{C}_V^{\pm 1} = -\sqrt{2} \frac{q(E_1 + E_2)}{m_1 + m_3} \gamma\phi_i \frac{\tau}{8\lambda} \left[\frac{\exp(\chi_i)}{\zeta_i^2} \left(1 - \frac{\chi_i - 2}{8\zeta_i k^2}\right) + \eta_i \frac{\exp(\chi_i')}{\zeta_i'^2} \left(1 - \frac{\chi_i' - 2}{8\zeta_i' k^2}\right) \right].$$

The required σ_{tot} are given by[16]

$$\sigma_{tot}(\pi p) = 23.4 + \frac{8.3}{M} \text{ mb},$$

and for the vector meson we adopt the form[17]

$$\sigma_{tot}(\rho p) = 0.27\left(98.6 + \frac{64.9}{M}\right)\frac{0.65}{(1 - t/m_\rho{}^2)^2} \text{ mb}.$$

For accuracy all the calculations of this paper were carried out[18] and plotted[19,20] by computer.

[1]P. Choudhury, K. J. M. Moriarty, J. H. Tabor, and A. Ungkitchanukit, Acta Phys. Austriaca. 48, 1 (1977).

[2]J. Pumplin, Phys. Rev. D 13, 1249, 1261 (1976).

[3]F. E. Paige and D. P. Sidhu, Phys. Rev. D 13, 3015 (1976); 14, 2307 (1976).

[4]L. Dick, A. Gonidec, A. Gsponer, M. Werlen, C. Caverzasio, K. Kuroda, A. Michalowicz, M. Poulet, D. Aschman, K. Green, P. Phizacklea, and G. L. Salmon, Phys. Lett. 57B, 93 (1975).

[5]H. D. I. Abarbanel and D. J. Gross, Phys. Rev. Lett. 26, 732 (1971); R. J. N. Phillips, G. A. Ringland, and R. P. Worden, Phys. Lett. 40B, 239 (1972); P. Salin and J. Soffer, Nucl. Phys. B71, 125 (1974).

[6]J. Soffer and D. Wray, Nucl. Phys. B73, 231 (1974).

[7]K. Ahmed, J. G. Körner, G. Kramer, and N. S. Craigie, Nucl. Phys. B108, 275 (1976).

[8]A. H. Mueller, Phys. Rev. D 2, 2963 (1970); 4, 150 (1971).

[9]S. A. Adjei, P. A. Collins, B. J. Hartley, K. J. M. Moriarty, and R. W. Moore, Ann. Phys. (N.Y.) 75, 405 (1973).

[10]F. C. Winkelmann, in *Experimental Meson Spectroscopy*—1974, proceedings of the Fourth International Conference, Boston, edited by D. A. Garelick (AIP, New York, 1974), p. 259. K. Böckmann, in *High Energy Physics*, proceedings of the Physical Society Conference, Palermo, 1975

[11]K. Paler *et al.*, Nucl. Phys. B96, 1 (1975).

[12]F. C. Winkelmann *et al.*, Phys. Lett. 56B, 101 (1975); D. Fong *et al.*, *ibid.* 60B, 124 (1975); M. Deutschmann *et al.*, Nucl. Phys. B103, 426 (1976); J. Brau *et al.*, *ibid.* B99, 232 (1975).

[13]J. Randa, Phys. Rev. D 7, 2236 (1973); Kyungsik Kang and P. Shen, *ibid.* 7, 164 (1973).

[14]J. Randa, Phys. Rev. D 9, 2612 (1974).

[15]N. S. Craigie, K. J. M. Moriarty, and J. H. Tabor, Phys. Rev. D 18, 590 (1978).

[16]V. S. Barashenkov, Interaction Cross Sections of Elementary Particles, Israel Program for Scientific Translations Ltd., 1968 (unpublished).

[17]J. J. Sakurai and D. Schildknecht, Phys. Lett. 40B, 121 (1972).

[18]K. J. M. Moriarty and J. H. Tabor, Comput. Phys. Commun. 12, 277 (1976).

[19]J. Anderson, K. J. M. Moriarty, and R. C. Beckwith, Comput. Phys. Commun. 9, 85 (1975).

[20]J. Anderson, R. C. Beckwith, K. J. M. Moriarty, and J. H. Tabor, Comput. Phys. Commun. (to be published).

FIG. 1. Diagrammatic representation of the Mueller generalized optical theorem.

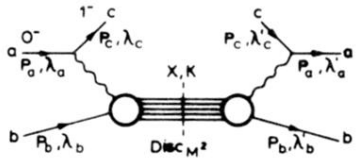

FIG. 2. The Mueller-Regge diagram for the production of vector mesons in the triple-Regge region but with the M^2-large condition relaxed.

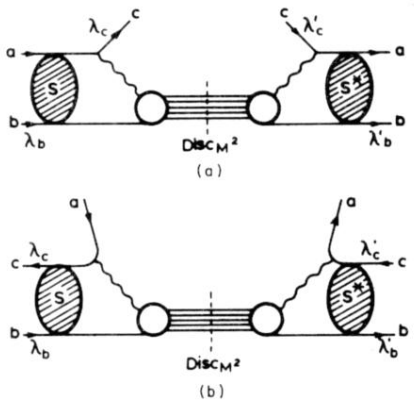

FIG. 3. (a) Rescattering correction to $0^- + p \to 1^- + X$ in the s channel. (b) Rescattering correction to $0^- + p \to 1^- + X$ in the $\bar{c}b$ channel.

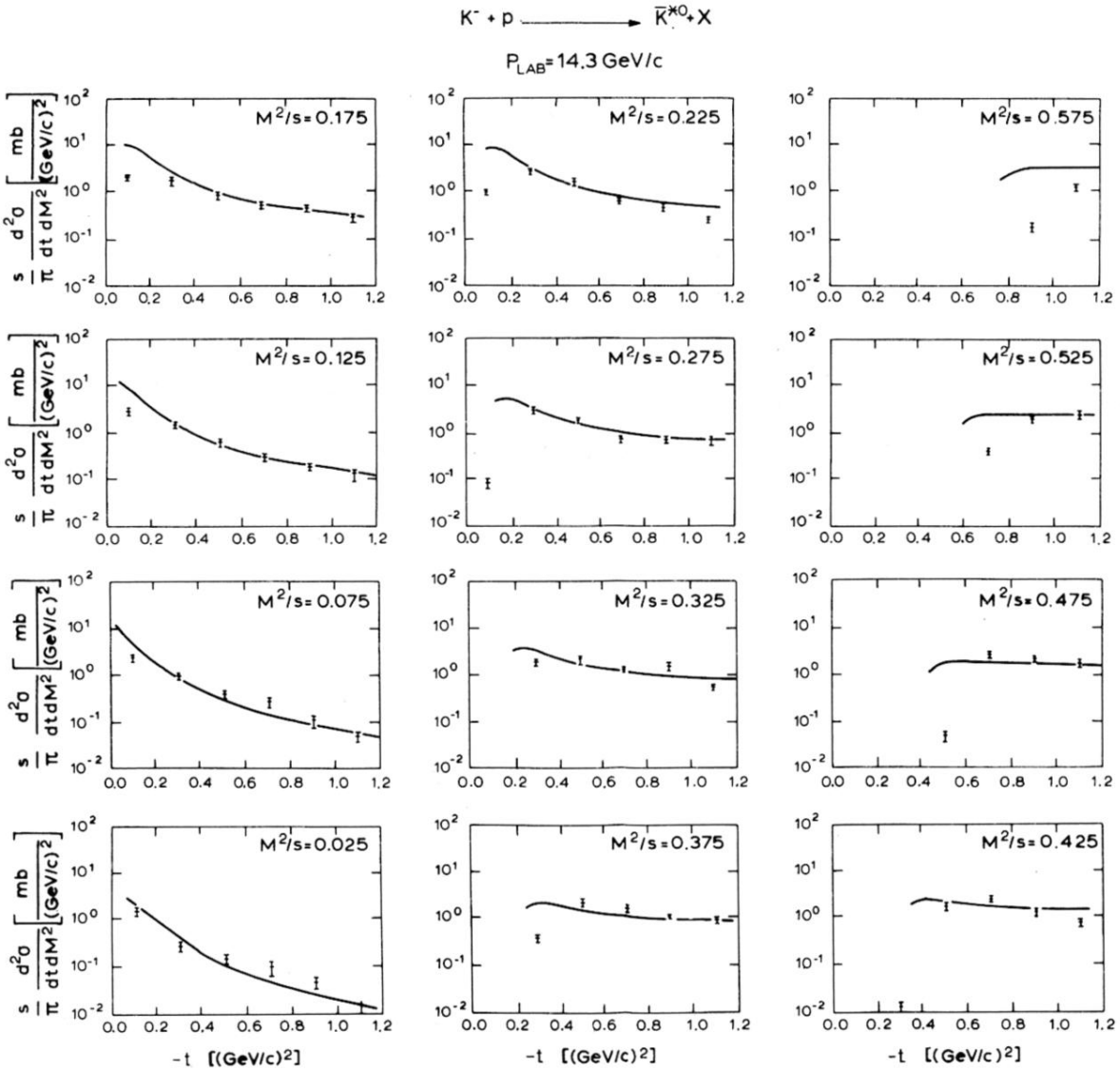

FIG. 4. The inclusive cross section for $K^- + p \to \bar{K}^{*0} + X$ for fixed M^2/s plotted vs t at 14.3 GeV/c. Data are from Ref. 11.

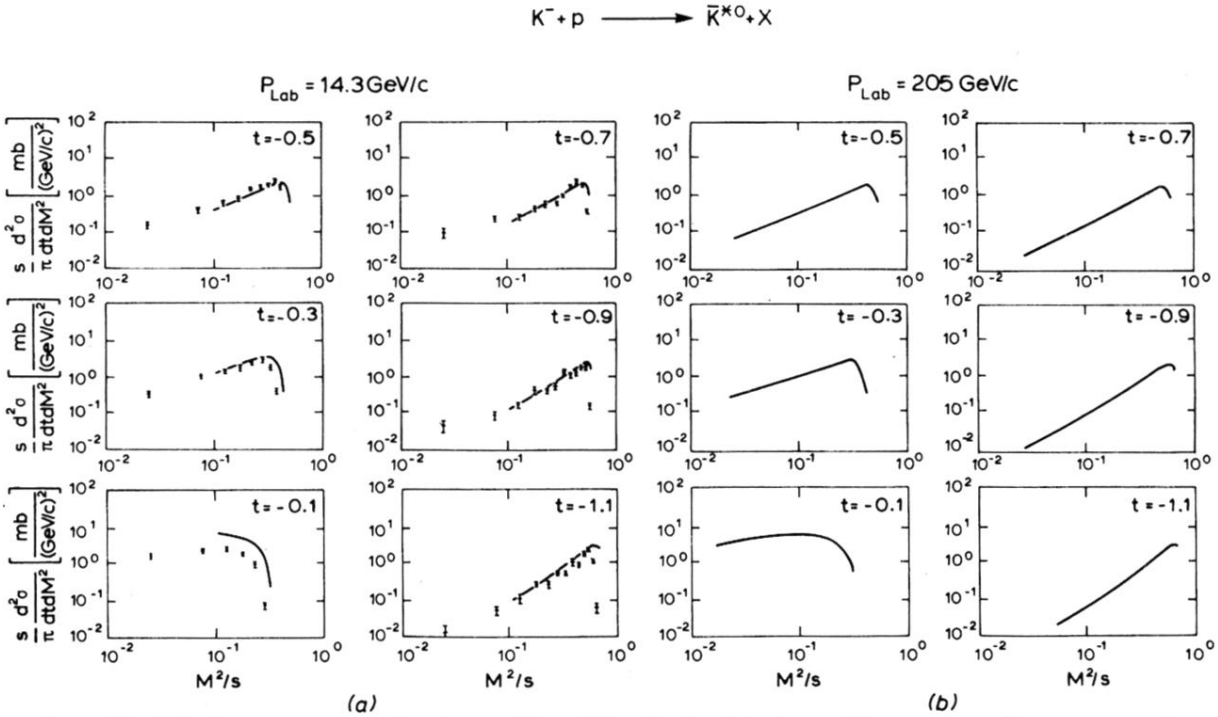

FIG. 5. The inclusive cross section for $K^- + p \to \bar{K}^{*0} + X$ for fixed t plotted vs M^2/s at 14.3 GeV/c and 205 GeV/c. Data at 14.3 GeV/c are from Ref. 11.

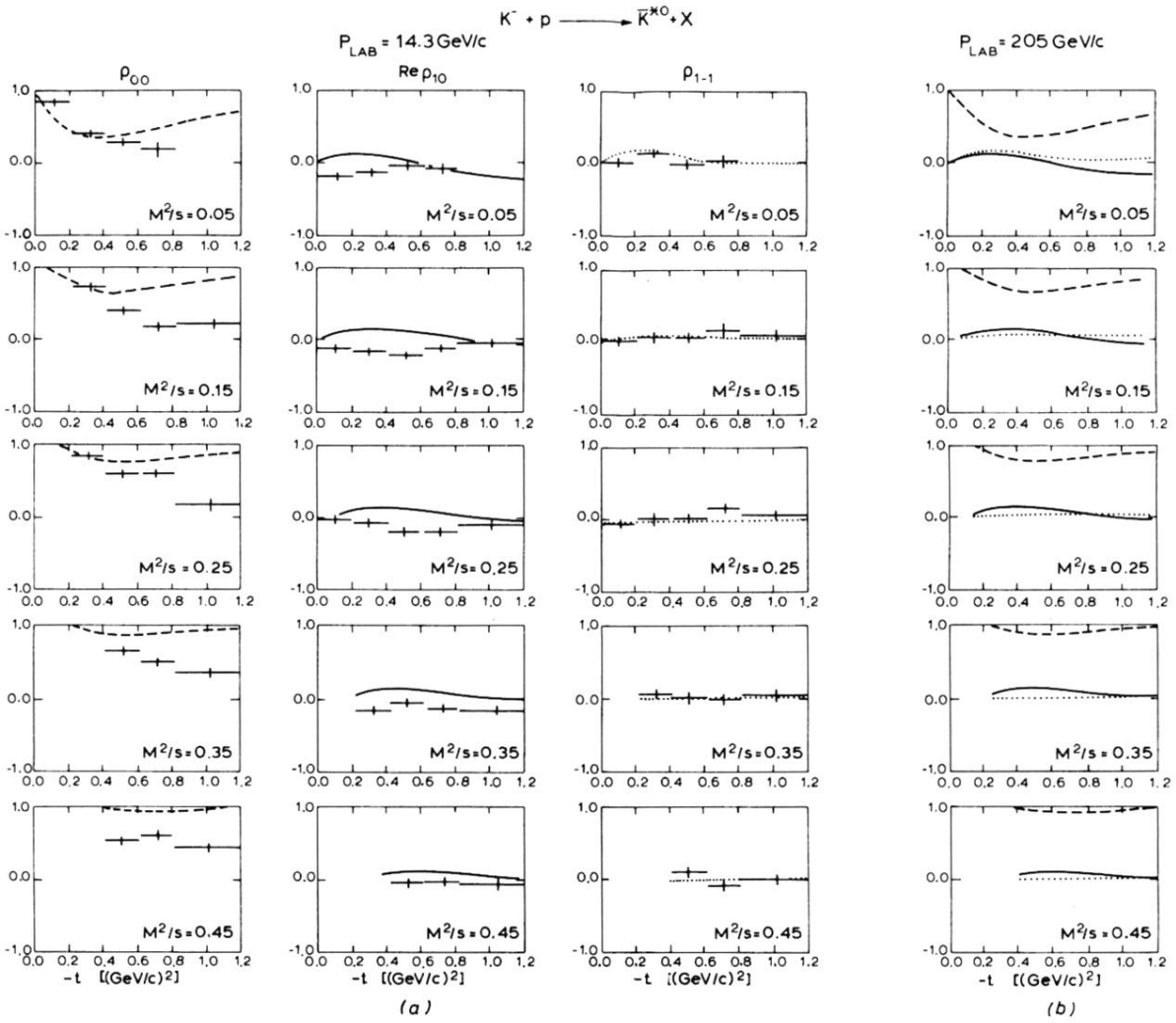

FIG. 6. The density matrix elements for the decay of the $\bar{K}^{*0}$ produced in the reaction $K^- + p \to \bar{K}^{*0} + X$ for fixed M^2/s plotted vs t in the Gottfried-Jackson frame at 14.3 GeV/c and 205 GeV/c. Data at 14.3 GeV/c are from Ref. 11.

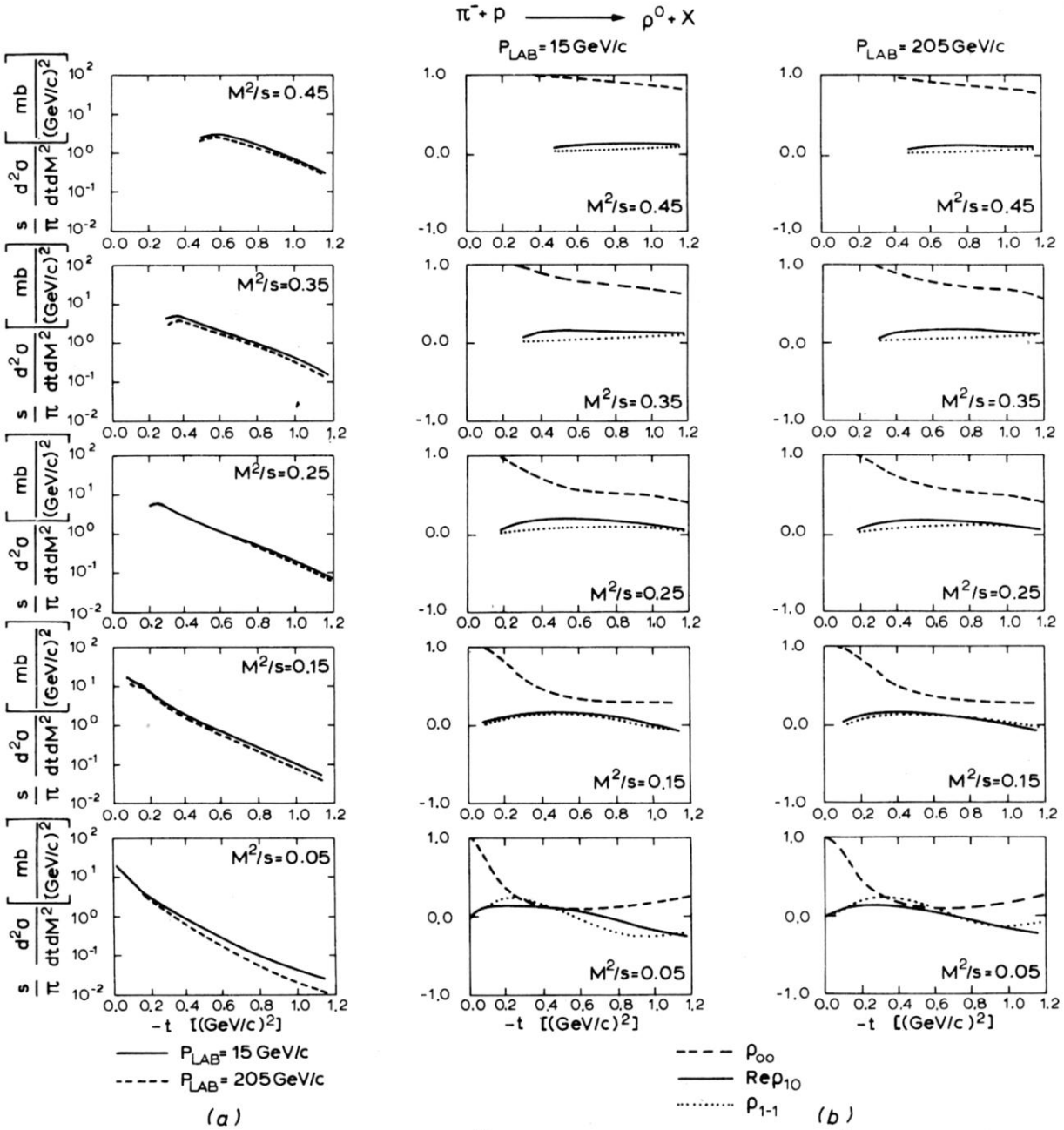

FIG. 7. (a) The inclusive cross section for fixed M^2/s plotted vs t for the reaction $\pi^- + p \to \rho^0 + X$ at 15 GeV/c and 205 GeV/c. (b) The density matrix elements for the decay of the ρ^0 produced in the reaction $\pi^- + p \to \rho^0 + X$ for fixed M^2/s plotted vs t at 15 GeV/c and 205 GeV/c.

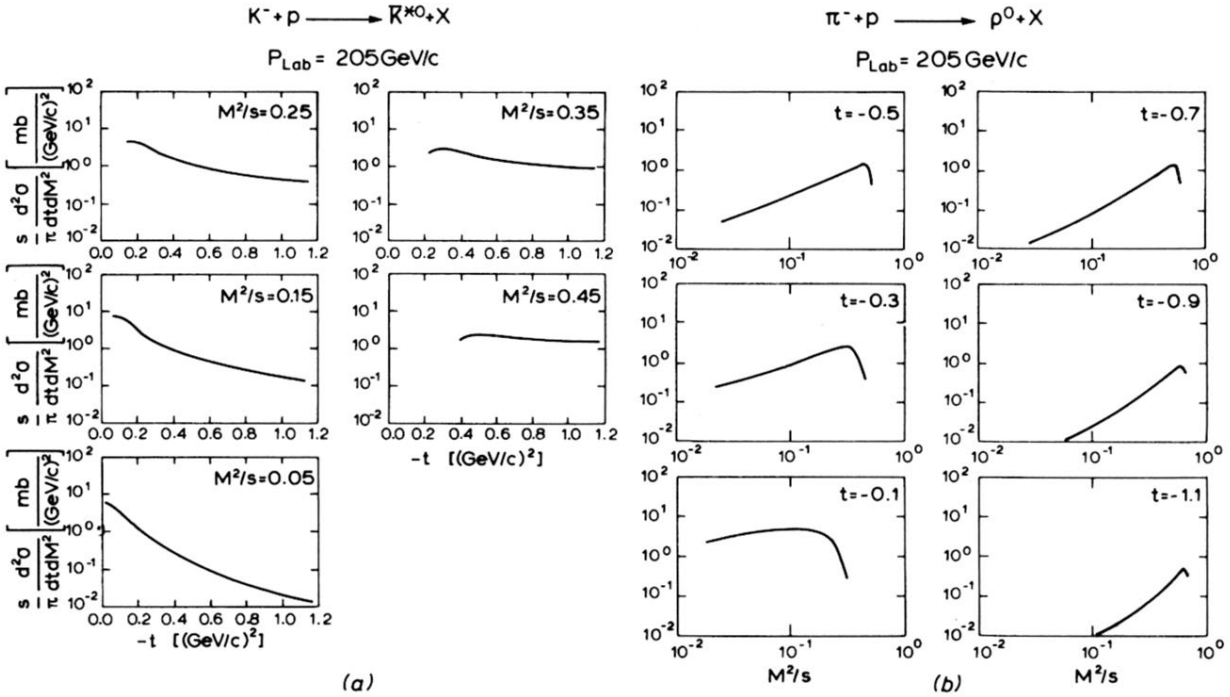

FIG. 8. (a) The inclusive cross section for $K^- + p \to \bar{K}^{*0} + X$ for fixed M^2/s plotted vs t at 205 GeV/c. (b) The inclusive cross section for $\pi^- + p \to \rho^0 + X$ for fixed t plotted vs M^2/s at 205 GeV/c.